Computers & Structures. Vol. 7, pp. 149–156. Pergamon Press 1977. Printed in Great Britain

NONLINEAR ANALYSIS OF REINFORCED CONCRETE STRUCTURES†

ORAL BUYUKOZTURK
Massachusetts Institute of Technology, Cambridge, MA 02139, U.S.A.

(*Received* 30 *November* 1975)

Abstract—For the prediction of yield and failure of concrete under combined stress, a generalization of the Mohr–Coulomb behavior is made in terms of the principal stress invariants. The generalized yield and failure criteria are developed to account for the two major sources of nonlinearity: the progressive cracking of concrete in tension, and the nonlinear response of concrete under multiaxial compression. Using these criteria, incremental stress–strain relationships are established in suitable form for the nonlinear finite element analysis.

For the analysis of reinforced concrete members by finite elements, a method is introduced by which the effect of reinforcement is directly included. With this approach, the stress–strain laws for the constituent materials of reinforced concrete are uncoupled permitting efficient and convenient implementation of a finite element program. The applicability of the method is shown on sample reinforced concrete analysis problems.

INTRODUCTION

Analytical procedures which may accurately determine stress and deformation states in reinforced concrete members are complicated due to many factors. Among them are (1) the nonlinear load–deformation response of concrete and difficulty in forming suitable constitutive relationships under combined stresses, (2) progressive cracking of concrete under increasing load and the complexity in formulating the failure behavior for various stress states, (3) consideration of steel reinforcement and the interaction between concrete and steel constituents that form the composite system and (4) time dependent effects such as creep and shrinkage of concrete.

Because of these complexities much of early analytical studies on reinforced concrete were based on either empirical approaches, using the results of large amounts of experiments, or on simple analysis assumptions such as the assumption of linear elastic behavior for the system. Indeed in the past the limitations imposed by classical analytical techniques have generally made such assumptions essential.

The development of numerical analysis methods, such as the finite element method[1, 2], permits realistic evaluation of internal stresses and displacements on which the limit requirements may be based for improved structural efficiency. Furthermore, such refined analytical solutions help in understanding and interpreting the observed behavior of structural elements from experiments.

The concept of using the finite element method for the analysis of concrete structures is rather new. In recent years there has been a growing interest in the application of the finite element procedure to the analysis of reinforced concrete structures, particularly with respect to the influence of cracking on the response. Scordelis[3] wrote a comprehensive survey of finite element analysis of reinforced concrete structures. Muto *et al.*[4] summarized further work in this area.

†Presented at the Second National Symposium on Computerized Structural Analysis and Design at the School of Engineering and Applied Science, George Washington University, Washington, D.C., 29–31 March 1976.

Success in developing finite element method for application to reinforced concrete[5–8] is closely linked to the development of quantitative information[9–11] on the load–deformation behavior of concrete. Formulation of such information in a suitable form for use in the analytical technique is essential. Despite intensive and continued research no universally accepted constitutive law exists which fully describes the concrete behavior in combined stress conditions.

The present study undertakes to (1) develop and verify the criteria for yielding and failure of concrete under combined stress states, (2) provide analytical means for direct modeling of reinforcement in the finite element analysis and (3) show the applicability of the method on sample reinforced concrete analysis problems.

The proposed yield and failure criteria account for the progressive cracking of concrete in tension, and the nonlinear response of concrete under multiaxial compression. These criteria are established without prior assumptions on the directional extent of cracking or yielding. They are used to establish incremental stress–strain relationships for use in the nonlinear finite element analysis. The verification of the yield and failure criteria of concrete is based on the biaxial stress states. However, the proposed invariant formulation for concrete behavior is general, and can accomodate changes to account for three-dimensional conditions upon availability of experimental data.

GENERALIZED MOHR–COULOMB BEHAVIOR

In the field of concrete research attempts have been made to apply some of the classical failure theories to concrete. These theories were altered however, to overcome some disadvantage or otherwise improve their agreement with the phenomenological behavior of concrete. New failure theories were therefore formed with specific application to concrete such as internal friction–maximum stress theory[12], octahedral shear-normal stress theory[13], Newman's two part criterion[14].

The octahedral shear-normal stress theory is a generalization of Mohr–Coulomb (internal friction) theory in that it includes the effect of the intermediate principal stress. A further generalization of the Mohr–Coulomb behavior

is possible by expressing the failure criterion in terms of the principal stress invariants[15]:

$$f(J_1, J_2) = 0 \tag{1}$$

where, using the summation convention

$$J_1 = \sigma_{ii}, \quad J_2 = \frac{1}{2} S_{ij} S_{ij} \tag{2}$$

and

$$S_{ij} = \sigma_{ij} - \frac{1}{3}\delta_{ij}\sigma_{kk} \tag{3}$$

(δ_{ij} is the Kronecker delta.)

The first invariant J_1 corresponds to the mean stress component of the stress state. The second invariant J_2 is a function of deviatoric stresses and hence excludes the effect of hydrostatic stress dependency. The most widely used yield conditions for ductile materials exclude the effect of the hydrostatic stress component and hence the first invariant J_1. However it is known that the mean stress has a significant role in discontinuity behavior and in eventual failure of concrete. Therefore, the first invariant, J_1, should be incorporated into the yielding and failure criteria for concrete.

The third plasticity invariant J_3 has been shown by Novozhilov[15] to represent the ratio of the mean shearing stress to the maximum shearing stress. This varies over very narrow limits. Therefore its effects on the formulation of a yielding or failure law would be of secondary importance. Consequently, it is possible for a brittle material like concrete, to write a yield or failure law in the form of eqn (1). The relationship expressed by eqn (1) will be termed "the generalized Mohr–Coulomb" law.

PROPOSED FAILURE LAW FOR CONCRETE

On the basis of the generalized Mohr–Coulomb behavior, together with the biaxial experimental data[10, 11], a failure law for concrete of the following form is proposed

$$3J_2 + \sqrt{(3)}\beta\sigma_0 J_1 + \alpha J_1^2 = \sigma_0^2 \tag{4}$$

where β, α and σ_0 are material constants. These constants are to be determined from the test data. For the concrete strength range used by Liu *et al.*[11] and Kupfer *et al.*[10], β, α and σ_0 constants were determined by a numerical trial procedure. The best fit was found by

$$\beta = \sqrt{(3)}, \quad \alpha = 1/5 \quad \text{and} \quad \sigma_0 = P/3. \tag{5}$$

With these values, the failure law eqn (4) becomes

$$3J_2 + PJ_1 + J_1^2/5 = P^2/9. \tag{6}$$

In a plane stress condition with principal stresses σ_1, and σ_2, the relationship for failure envelope is

$$27(2k^2 - k + 2)\sigma_1^2 + 45P(1 + k)\sigma_1 - 5P^2 = 0 \tag{7}$$

where $k = \sigma_2/\sigma_1$; $k = 0$ corresponds to the uniaxial case in the first principal direction. This failure envelope is plotted in a dimensionless principal stress coordinate system in Fig. 1. Equation (7), as a whole, represents an ellipse rotated and shifted with respect to the principal

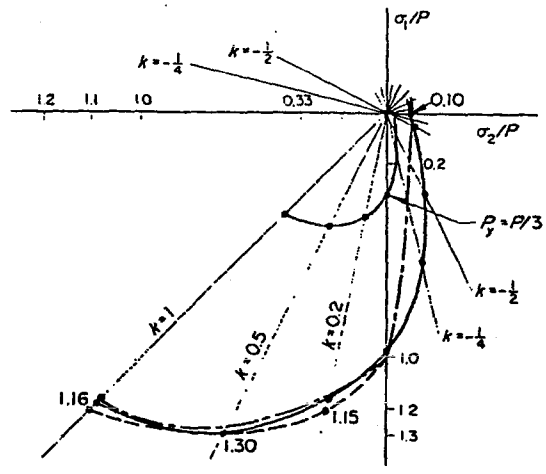

Fig. 1. Analytical and experimental failure envelopes for concrete. ———, Kupfer and Hilsdorf[10]; – – – –, Liu, Nilson, and Slate[11]; ———, Present formulation.

$$3J_2 + \sqrt{(3)}\beta\sigma_0 J_1 + \alpha J_1^2 = \sigma_0^2$$
$$(\beta = \sqrt{(3)}\sigma_0 = 1/3P\alpha = 1/5)$$

axes. The resulting envelope has a distorted shape with a small tension–tension zone, a narrow tension–compression zone and a highly expanded compression–compression area.

In general, a satisfactory agreement is seen between the test data and the assumed failure function. The comparison of the proposed failure envelope with the experiment is made for three different principal stress zones:

(1) *Compression–compression zone*

The strength ratio σ_1/P was calculated from eqn (7) for various k values. A strength increase of 15, 30 and 16% was obtained for the principal stress ratios of $k = 0.2$, $k = 0.5$ and $k = 1.0$ respectively. These values are in good agreement with the test data[10, 11]. In the analysis, this portion of the failure envelope is assumed to determine a "crushing" type of failure of the material. Here, the term "crushing" is used to express the failure of concrete under compression stress in the plane of the material model.

It is noted that, with sufficient experimental information, a failure law based on critical local deformations[16] or limit strains may be incorporated with eqn (6) to constitute a dual failure criterion similar to that described by Newman[14]. However, at the present time it appears that the limiting strain or deformation proposals are not general enough to provide a quantitatively adequate criterion for formulation.

(2) *Tension–compression zone*

From Fig. 1 it is seen that in tension–compression zone, the analytical failure envelope deviates from the test data. This deviation is pronounced in the σ_2 tension direction between the two extreme uniaxial cases. For the uniaxial case $k = 0$ two extreme values for σ_1 are found; from eqn (7) the first is $\sigma_1 = P$ (uniaxial compressive strength) and the second is $\sigma_1 = 0.10P$ (uniaxial tensile strength). Therefore the extreme values are in agreement with the actual tests. Consistent with the experiments, these two extreme points are connected by a straight line for failure in the tension–compression range (Fig. 2). It should be noted that in this stress zone, with σ_2 tensile stresses of

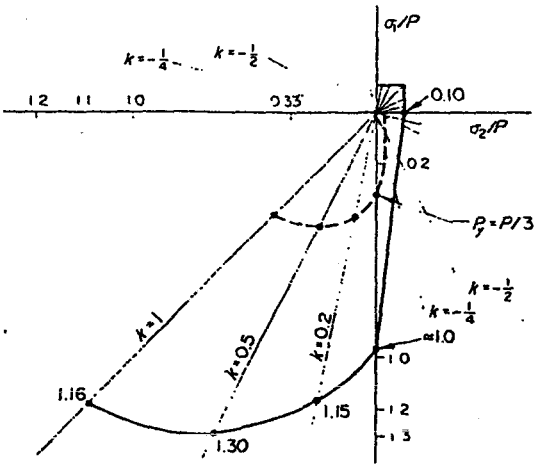

Fig. 2. Yield and failure criteria assumed in the analysis. ——, Failure envelope; – – – –, Yield envelope.

sufficient magnitude as defined by that straight line, cracking will occur. Subsequent loading, then, will give rise to the compressive stress, σ_1, until crushing occurs in the σ_1 direction.

(3) *Tension–tension zone*

In the tension–tension zone the stress–strain behavior is linear elastic and failure occurs by cracking. The maximum stress (or strain) criterion is used to determine cracking with uniaxial tensile strength (or strain) as the limiting value. The tensile strength of concrete may vary depending upon the concrete mixture. For the present study $0.10P$ was assumed for tensile strength of concrete and the resulting failure envelope is shown in Fig. 2.

PROPOSED YIELD LAW FOR CONCRETE

Up to about 30–35% of the compressive strength, concrete under uniaxial compression behaves as linear elastic. In biaxial loading, the elastic range in the compression–compression zone expands due to the microcracking confinement[7, 11] caused by lateral restraint. The magnitude of this expansion is a function of the principal stress ratio in a similar way as in the strength increase due to lateral confinement. The yield surface is therefore obtained by simply scaling the failure envelope down to a size where uniaxial yield point corresponds to about one-third of the uniaxial compressive strength.

The general failure surface eqn (4) and eqn (6), with given material constants, may easily be modified to formulate the yield surface. This gives the following:

$$3J_2 + \bar{\sigma}J_1 + J_1^2/5 = \bar{\sigma}^2/9 \tag{8}$$

where

$$\bar{\sigma} = P_y = \frac{1}{3}P \quad \text{(compression)}, \quad \bar{\sigma} > 0.$$

This yield surface is plotted in dimensionless principal stress space on Fig. 2.

As discussed in the previous section, for the tension–compression zone, the envelope expressed by eqn (8) deviates slightly from the tests; the test data produces a relationship close to a straight line in this zone. However, it will be assumed that the differences between eqn (8) and the linear relationship for this zone is not important. This assumption is based on the fact that:

(1) for small tensile σ_2 values, the effect of σ_2 on the nonlinearity is negligible,

(2) for relatively large tensile σ_2 values, the behavior is governed by cracking in orthogonal planes parallel to the compressive σ_1 direction[11]. Therefore, with vanishing σ_2 values upon cracking, yield criterion reduces to a one-dimensional yield formulation with nonlinearities introduced in the compressive σ_1 direction only.

In the present study, therefore, the yield condition expressed by eqn (8) is used for both compression–compression and the tension–compression zones. This maintains the continuity of the yield surface.

In the tension–tension zone, consistent with the experiments[10, 17] a linear elastic behavior is assumed with elastic slope equal to the initial tangent modulus in uniaxial compression.

The utilization of stress invariants in formulating the yielding of concrete is particularly attractive because, as mentioned earlier, such formulation provides a physical interpretation in terms of deviatoric and hydrostatic stress component effects. Furthermore, a yield condition based on the stress invariants permits convenient use of the incremental plasticity approach for analyses with material nonlinearities.

INCREMENTAL STRESS–STRAIN RELATIONSHIPS FOR THE ELASTIC–PLASTIC BEHAVIOR

In constructing the relationship between stress and strain in the inelastic range for multiaxial stress states, one must define (a) the condition for yield, (b) the general form of the desired stress–strain law and (c) a criterion for work hardening. With these determined, the objective is to establish the Prandtl–Reuss relations in an incremental form.

The yield condition eqn (8) can be rewritten as follows,

$$f = 3(3J_2 + \bar{\sigma}J_1 + J_1^2/5)^{1/2} = \bar{\sigma} \tag{9}$$

where $\bar{\sigma}$ represents the "equivalent stress" which is defined to be able to extrapolate from a simple uniaxial compression test into the multi-dimensional situation. The initial yield occurs, when the equivalent stress, $\bar{\sigma}$, equals the yield stress P_y measured in the uniaxial compression test. With loading continued, the subsequent yielding occurs and plastic strains are introduced. For each value of equivalent strain, $\bar{\epsilon}^p$, there corresponds an equivalent stress. The equivalent strain can be directly obtained from uniaxial compressive curve by subtracting the elastic strains.

The slope of $(\bar{\sigma}, \bar{\epsilon}^p)$ curve, H', is known as hardening coefficient. From that curve one can write:

$$d\bar{\sigma} = H' \, d\bar{\epsilon}^p. \tag{10}$$

On the other hand, from eqn (9), the total differential df can be written as:

$$\left[\frac{\partial f}{\partial \sigma}\right]\{d\sigma\} + \frac{\partial f}{\partial \bar{\sigma}} d\bar{\sigma} = d\bar{\sigma} \tag{11}$$

or

$$\left[\frac{\partial f}{\partial \sigma}\right]\{d\sigma\} + \frac{3J_1}{2\bar{\sigma}} d\bar{\sigma} = d\bar{\sigma}. \tag{12}$$

Rearranging, and with the use of eqn (10) one obtains

$$\left[\frac{\partial f}{\partial \sigma}\right]\{d\sigma\} = \left(1 - \frac{3J_1}{2\bar{\sigma}}\right) H' \, d\bar{\epsilon}^p. \tag{13}$$

For the flow rule of the multiaxial plasticity, usual Prandtl–Reuss representation, with isotropic hardening is employed. Isotropic hardening simply implies a uniform expansion of the yield surface in all stresses. That is, by the occurrence of plastic strains the yield surface grows in size with the same shape as in the initial yield conditions. The flow rule is:

$$\{d\epsilon^p\} = d\bar{\epsilon}^p \left\{\frac{\partial f}{\partial \sigma}\right\}. \tag{14}$$

Because the elastic components of strains are only strains that can be associated with changes in stresses, the increment of stress is related to the increment of elastic strain by

$$\{d\sigma\} = [C]\{d\epsilon^e\} \tag{15}$$

where $[C]$ is the elastic strain to stress transformation matrix. With elastic–plastic strain decomposition

$$\{d\sigma\} = [C](\{d\epsilon\} - \{d\epsilon^p\}) \tag{16}$$

where

$\{d\epsilon\}$ = increment of total strain vector.

Substituting eqn (14) into eqn (16), and using eqn (13), the required incremental stress–strain relation is obtained

$$\{d\sigma\} = \left[[C] - \frac{[C]\left\{\frac{\partial f}{\partial \sigma}\right\}\left[\frac{\partial f}{\partial \sigma}\right][C]}{\left(1 - \frac{3J_1}{2\bar{\sigma}}\right)H' + \left[\frac{\partial f}{\partial \sigma}\right][C]\left\{\frac{\partial f}{\partial \sigma}\right\}}\right]\{d\epsilon\} \tag{17}$$

or

$$\{d\sigma\} = [D]\{d\epsilon\} \tag{18}$$

where $[D]$ is the elastic–plastic incremental strain to stress transformation matrix. It is seen that $[D]$ is symmetric. Note that the hardening coefficient multiplier $(1 - 3J_1/2\bar{\sigma})$ cannot be zero since the substitution of this condition in eqn (8) results in a negative J_2 value. In the case of perfect plasticity the hardening coefficient H' is zero. As seen from eqn (17) this does not cause any numerical difficulty since C is nonsingular.

EFFECT OF MICROCRACK CONFINEMENT ON ISOTROPIC WORK HARDENING

The stiffening effect of biaxiality [7, 11] on the deformation of concrete is represented by the elastic portion of the constitutive relationship $[C]$ in eqn (17). This is done by introducing the directional equivalent tangent moduli in principal stress space and incorporating them into $[C]$. In the elastic–plastic range, however, this plastic portion of the constitutive matrix is based on H' hardening coefficients which are taken from uniaxial compression tests.

The variation of the hardening coefficients as a function of the principal stress ratio may be taken into consideration in the incremental scheme. Such procedure would utilize H'_b effective hardening coefficients for a given stress state (Fig. 3). The procedure would involve simply replacing H' coefficients in eqn (17) by the H'_b effective values for the stress combination corresponding to the load increment considered.

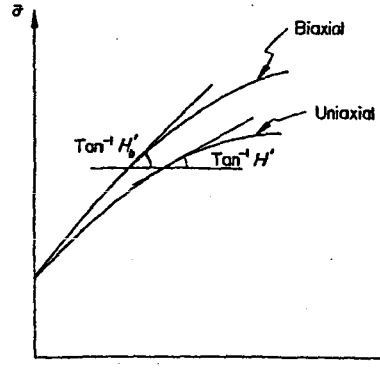

Fig. 3. Effective hardening coefficients for biaxiality.

PROGRESSIVE CRACKLING

Internal stresses and deformations as well as external deflections are highly affected by cracking. Cracks develop first in relatively weak regions of the structural system. As the external load is increased, new cracks form in other regions as already developed cracks propagate within the system. In order to incorporate the phenomenon of progressive cracking in the analysis, as cracks occur, the topology of the model should be redefined and analysis should continue with this newly modified system. This is done by using the element representation of cracks [18] in the model, and marching out incrementally.

The stress is converted to principal stresses at various angles to the global axes. If the stress state at an integration point of an element meets the failure criteria, then a crack is defined at that point, the crack being oriented perpendicular to the principal tension direction. To account for the presence of the crack in succeeding increments of loading, the incremental constitutive matrix $[D]$ is modified by setting appropriate terms to zero such that at that point the element cannot transmit tensile stresses normal to the crack direction. Thus, the crack propagation is established without prior assumptions on the directional extent of cracking. Note that a proportion of the shear modulus may be retained in $[D]$ to account for the aggregate interlocking.

EFFECT OF REINFORCEMENT

Since concrete is mostly used in conjunction with steel reinforcement, an accurate analysis requires the consideration of the members forming the composite structure. In the present analysis of reinforced concrete members by finite elements, a method has been introduced by which the effect of reinforcement is directly included. In the model, at each physical location of the structure, two geometrically identical finite elements are used. The first (concrete element), represents the concrete and is a "full" element. The second (rebar element) is basically an empty block element containing reinforcing bars running in prescribed directions simulating the actual reinforcement configuration (Fig. 4a). The strain compatibility between steel and concrete is maintained by using the same shape functions for both elements.

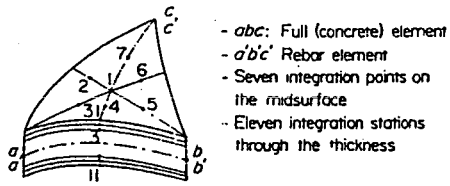

(a) Doubly-curved isoparametric composite element

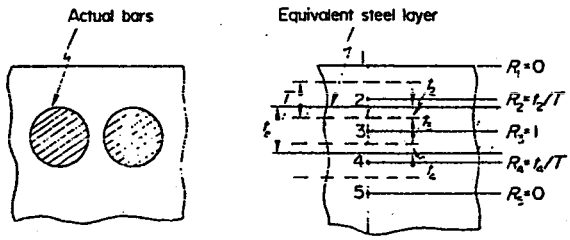

(b) Equivalent reinforcement

Fig. 4. Reinforcement representation in the analytical model.

With this approach, the stress–strain laws for constituent materials of reinforced concrete are uncoupled permitting efficient and convenient implementation in a finite element program. In addition, the method proves convenient to investigate the relative contributions of the concrete and steel components in resisting loads. The approach is applicable to two and three-dimensional models. Also, the reinforcement, in the rebar element, can be represented as discrete bars or as smeared steel layers (sheets) with equivalent thicknesses.

In the present work the application of the method is demonstrated by the use of doubly-curved isoparametric thin shell elements[19]. The following assumptions are made:

(1) The actual reinforcing bars are represented by equivalent anisotropic steel layers by making appropriate adjustments to $[D]$ matrix for the rebar element. These layers carry uniaxial stress only in the same direction as the actual bars. Dowel action is neglected.

(2) Strain compatibility between steel and concrete is maintained. This condition implies that there is a sufficiently strong bond between the two materials so that no relative movement of the steel and the surrounding concrete can occur.

It is known that for plates and shells, piecewise generalized stress–strain relations are defined by integrating through the thickness. For this analysis it is necessary to use incremental stress–strain relationship of the type expressed by eqn (18). For a full (concrete) element the generalized stress–strain relationship is

$$\begin{Bmatrix} dN \\ dM \end{Bmatrix} = \int_{-H/2}^{H/2} \begin{bmatrix} [M] & [M]h \\ [M]h & [M]h^2 \end{bmatrix} \begin{Bmatrix} d\epsilon_0 \\ dk \end{Bmatrix} dh \qquad (19)$$

where

dN = the increment of direct stress resultant
dM = the increment of bending stress resultant
$d\epsilon_0$ = mid-wall component of strain increment
dk = bending component of the strain increment
H = the wall thickness.

At each integration point of the element the shell wall is divided into a number of stations with constant intervals, T, through the thickness (Fig. 4a). Using $[D]$, the matrix $[M]$ is evaluated at the start of each increment and for each of the stations.

For the rebar element, based on the actual area of reinforcing bars, an equivalent thickness t_e is calculated for each layer through the thickness. For a steel layer with anisotropic properties consistent with uniaxial condition (to represent the reinforcing bars),

$$d\sigma_i = (R_i D_i)\, d\epsilon_i. \qquad (20)$$

Here $R_i = t_i/T$ where t_i is the portion of the equivalent steel area contributed to the ith integration station. Figure 4b shows the ratios R_i for a rebar element with one layer. For each integration station the R_i values are substituted in $[D]$ in the local coordinate system consistent with the uniaxial reinforcement direction.

The generalized stress–strain relation at station i then becomes

$$\begin{Bmatrix} dN \\ dM \end{Bmatrix} = \int_{-H/2}^{H/2} \begin{bmatrix} R_i D_i & R_i D_i h \\ R_i D_i h & R_i D_i h^2 \end{bmatrix} \begin{Bmatrix} d\epsilon \\ dk \end{Bmatrix} dh. \qquad (21)$$

This integral is easily formed by numerical integration using the constant interval T. Note that for integration stations with no reinforcement contribution, the R_i multipliers will be zero.

SAMPLE PROBLEMS

The technique developed for the failure analysis of reinforced concrete members has been implemented in a nonlinear finite element program[20]. The applicability of the method is demonstrated by two numerical examples using the doubly-curved isoparametric thin shell elements.

Deep beam example

The model of a reinforced concrete deep beam selected for analysis is shown in Fig. 5. This beam corresponds to Leonhardt's test specimen WT3 and is fully described in[21]. The stress–strain curves of this concrete along with the curve fit for this analysis, are shown in Fig. 6. Uniaxial compressive strength of concrete was 302 kg/cm². The modulus of rupture was 48 kg/cm².

The reinforcement was affected at the bottom portion of the beam by two steel layers with equivalent thicknesses $t_e = 0.107$ cm on each face. The symmetry permitted the study of only one half of the beam.

At about 37% of ultimate load yielding occured in the support area. And at 55% of ultimate load first tension cracks occurred at the bottom of the beam. As loads were increased further yielding and cracking occurred as seen in Fig. 7. The ultimate strength was reached at 120 tons when material instability was obtained due to yielding and cracking in the support areas.

Predictions of the analysis for the initiation and propagation of cracks, and the deformation behavior are in good agreement with experimental observation[21]. Analytical deflections and failure load are slightly smaller than those from the tests (Fig. 8). (The predicted failure load is about 7% less than the reported experimental value.) The differences between the analytical and the experimental results are within the scatter in the reported test data.

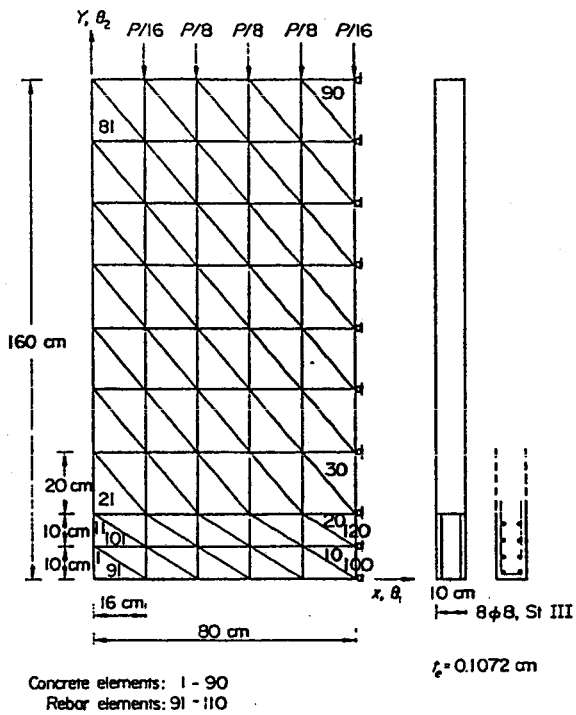

Fig. 5. The deep beam model.

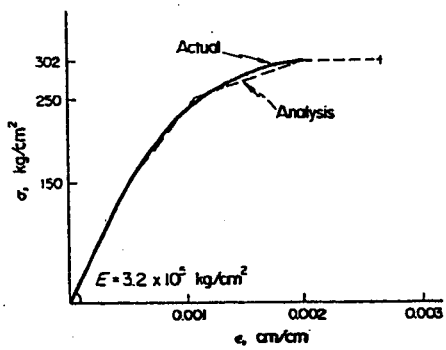

Fig. 6. Stress–strain curve of concrete.

Cylindrical shell roof example

Figure 9 shows the model of the barrel vault problem studied. The uniaxial compressive strength of concrete was 250 kg/cm². The assumed compressive stress–strain curve was similar to that shown in Fig. 6 with an initial elastic modulus of 2.1×10^5 kg/cm². Modulus of rupture was assumed to be one-tenth of the compressive strength. Steel reinforcements was assumed to be at 0.6% distributed evenly between the two shell surfaces. The reinforcements were assumed to have equivalent thicknesses with uniform stiffness in both orthogonal directions with no shear effects.

A load of 0.015 kg/cm² caused tensile failures at elements 1, 8 and 16. (In the analysis half the elastic shear modulus was retained for cracked elements to effect the agregate interlocking in concrete.) The crack propagation with increasing loads is shown in Fig. 10. The load deflection results for the mid-point of the edge of the shell, together with the elastic solution given by Scordelis and Lo [22], is shown in Fig. 11. The effect of cracking is highly pronounced in this curve showing severe nonlinearity from the early stages of loading.

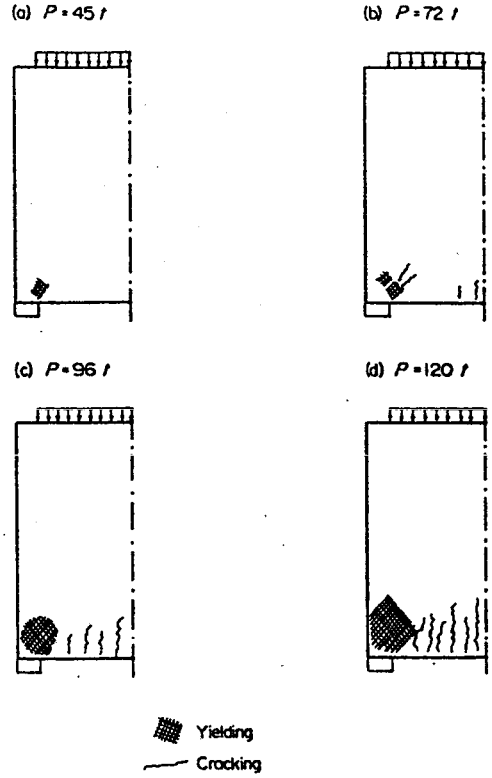

Fig. 7. Predicted yielding and cracking of the beam.

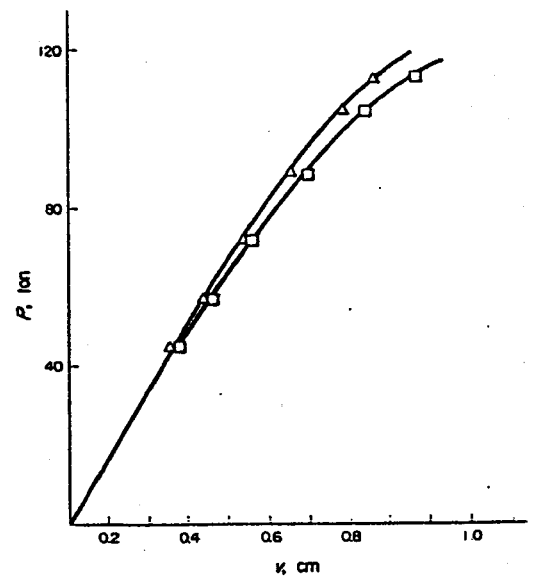

Fig. 8. Vertical deflections at the mid span of the beam. —Δ—Δ—, Analysis; —□—□—, Test [21].

CONCLUSION

Using the finite element method of analysis, modified as dictated by the particular properties of reinforced concrete, an analytical model is given which permits the detailed study of structural behavior through the entire range of loading.

Adequate comparisons between analysis and tests are achieved using the criterion for yielding and failure of concrete, expressed in terms of stress invariants.

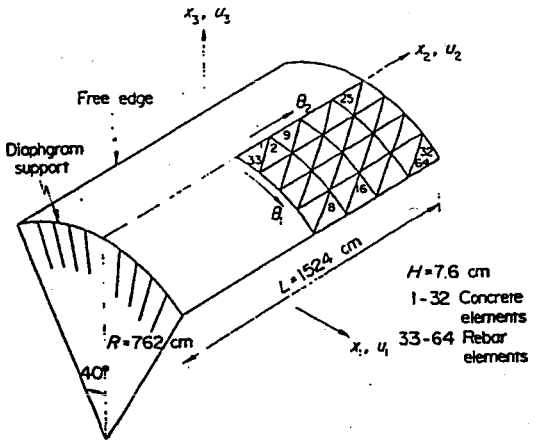

Fig. 9. The reinforced concrete roof model.

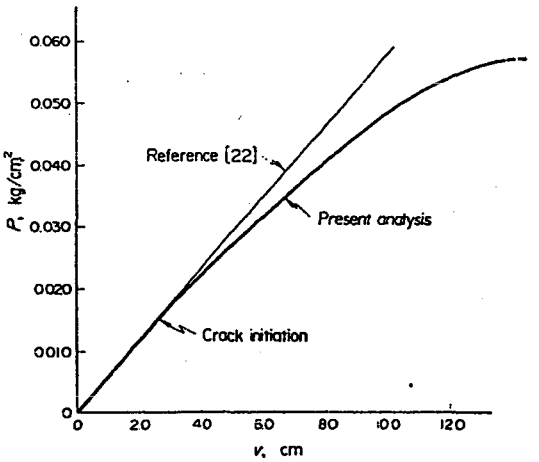

Fig. 11. Vertical deflection at mid point of the free edge.

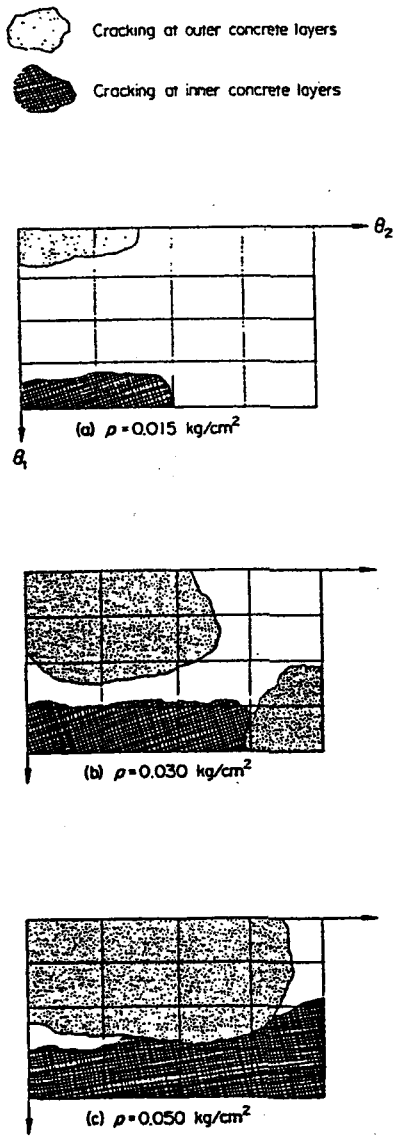

Fig. 10. Predicted cracking in the shell roof.

This study suggests that the model provides a powerful basis for analysis which promises to give new insight into the performance of reinforced concrete.

REFERENCES

1. O. C. Zienkiewicz. *The Finite Element Method in Engineering Science.* McGraw-Hill, New York (1971).
2. R. H. Gallagher. *Finite Element Analysis—Fundamentals.* Prentice Hall Civil Engineering and Engineering Mechanics Series, New York (1975).
3. A. C. Scordelis. Finite element analysis of reinforced concrete structures. *Proc. Specialty Conference on the Finite Element Method in Civil Engng,* pp. 71–113. McGill University, Montreal, Canada (June 1972).
4. K. Muto, N. Ohmori, T. Sugano, T. Miyashita and H. Shimizu, Nonlinear analysis of reinforced concrete buildings. *Proc. Tokyo Seminar on Finite Element Analysis.* University of Tokyo Press (1973).
5. D. Ngo and A. C. Scordelis, Finite element analysis of reinforced concrete beams. *ACI J. Proc.* 64(3) (Mar. 1967).
6. A. H. Nilson, Nonlinear analysis of reinforced concrete by the finite element method. *ACI J. Proc.* 65(9) (Sept. 1968).
7. O. Buyukozturk, A. H. Nilson and F. O. Slate, Stress–strain response and fracture of a concrete model in biaxial loading. *ACI J. Proc.* 68(8) 540–599 (Aug. 1971).
8. M. Suidan and W. C. Schnobrich, Finite element analysis of reinforced concrete. *J. Struct. Div. ASCE,* ST10, 2109–2122 (Oct. 1973).
9. H. Weigler and C. Becker, Untersuchuhgen uber das Bruch und Verformungsverhalten von Beton bei zweiachsiger Beanspruching. *Heft* 157 *des Deutschen Ausschusses fur Stahlbeton,* Berlin (1963).
10. H. Kupfer, H. K. Hilsdorf and H. Rusch, Behavior of concrete under biaxial stresses. *ACI J. Proc.* 66(8), 656–666 (Aug. 1969).
11. T. C. Y. Liu, A. H. Nilson and F. O. Slate, Stress–strain response and fracture of concrete in uniaxial and biaxial compression. *ACI J., Proc.* 69(5) 291–295 (May 1972).
12. H. J. Cowan, The strength of plain, reinforced and prestressed concrete under the action of combined stresses. *Magazine of Conc. Res.* 5(14) 75–86 (Dec. 1953).
13. B. Bresler and K. S. Pister, Failure of plain concrete under combined stresses. *Proc., ASCE* 81(674) (Apr. 1955).
14. K. Newman and J. B. Newman, Failure theories and design criteria for plain concrete. *Proc. Southampton* 1969 *Civil Engng Materials Conf.* (Edited by M. Teleni), pp. 963–993. Wiley Interscience, London (1974).
15. V. V. Novozhilov, The physical meaning of the stress invariants of the theory of plasticity (in Russian), *Applied Mathematics and Mechanics* (Published by the Academy of Science, USSR), 16, 617–619 (1952).

16. F. O. Slate and B. L. Meyers, Deformations of plain concrete. Paper presented at the *5th Inter. Symp. Chem. of Cement*, Tokyo (Oct. 1968).
17. J. C. Carino, The behavior of a model of plain concrete subject to compression–tension and tension–tension biaxial stresses. *Rep.* No. 357, Dept. of Structural Engineering, Cornell University (July 1974).
18. O. Buyukozturk and A. H. Nilson, Finite element analysis of a model of plain concrete with biaxial loads. Proc., *Specialty Conference on The Finite Element Method in Civil Engng*, pp. 703–728. McGill University, Montreal, Canada (June 1972).
19. G. A. Dupuis, Application of Ritz method to thin elastic shell analysis. Brown University Engineering Department, *Rep.* No. 0014–008/1 (1970).
20. P. V. Marcal, On general purpose programs for finite element analysis, with special reference to geometric and material nonlinearities. Paper presented at the *Symp. Numer. Solution of Partial Differential Equations*, University of Maryland (May 1970).
21. F. Leonhardt and R. Walther, Wandertige trager. *Deutscher Ausschuss Fur Stahlbeton*, Heft 178, Berlin (1966).
22. A. C. Scordelis and K. S. Lo, Computer analysis of cylindrical shells. *ACI J., Proc.* 16(5) 539–561 (May 1964).